

Highly accurate potential energy curves for the hydrogen molecule ion

Francisco M. Fernández and Javier Garcia*

INIFTA, DQT, Diagonal 113 y 64 S/N 1900 La Plata, Argentina

Potential energy surfaces of the hydrogen molecular ion H_2^+ in the Born-Oppenheimer approximation are computed by means of the Riccati-Padé method (RPM). The convergence properties of the method are analyzed for different states. The equilibrium internuclear distance, as well as the corresponding electronic plus nuclear energy, and the associated separation constants, are computed to 40 digits of accuracy for several bound states. For the ground state the same parameters are computed with more than 100 digits of accuracy. Additional benchmark values of the electronic energy at different internuclear distances are given for several additional states. The software implementation of the RPM is given under a free software license. The results obtained in the present work are the most accurate available so far, and further additional benchmarks are made available through the software provided.

arXiv:2107.01228v1 [physics.chem-ph] 2 Jul 2021

* jgarcia@fisica.unlp.edu.ar

I. INTRODUCTION

The hydrogen-ion molecule H_2^+ is the simplest molecule that exists in Nature, and, after applying the Born-Oppenheimer approximation, the solution of the Schrödinger equation becomes one of the simplest non-trivial problems in quantum mechanics. The Schrödinger equation is separable into two one-dimensional equations that depend on the electronic energy, the internuclear distance, and a separation constant, and the relative ease of their solution led to excellent analyses of the H_2^+ spectrum as early as the 1950s [1–5]. These efforts are nothing short of remarkable, given the time period they were performed at, but due to the obvious limitations imposed by the computing power available at the time, the tabulated spectra were computed using double precision, meaning that they contain at most 15 significant digits.

In general, more accurate computations of the eigenspectra of quantum-mechanical problems are of interest for testing other computational methods (see, for example, the recent discussion in Refs. [6] and [7]). The H_2^+ system is of particular interest since, as it involves a real molecule, it is useful not only to provide benchmark values for testing numerical methods [8] in general, but also for and quantum-chemical methods, such as those based on perturbation theory [9–11], or the variational theorem [12, 13]. It has also been used to validate potential energy surfaces (PESs) [14, 15], which are of the utmost importance in the computation of condensed matter properties [16, 17]. The computed spectra and PESs of H_2^+ have also been used to model covalent bonding [18], and in experimental observations of molecular properties [19–21]. Both the lower- and higher-lying states of the H_2^+ have been recently computed using semiclassical approximations [22–24], and variational approaches [25]. The solutions of the H_2^+ molecule ion problem have been also analyzed in terms of hypergeometric functions [26], the Heun confluent functions [27, 28], and Coulomb Sturmians [29, 30]. Series solutions have also been given for the spectrum of H_2^+ [31].

Upon thorough inspection of the literature surveyed here, it is found that all the tabulated spectra contain at most 15 significant digits, which is a product of the limitation of floating point calculations. Some of the references cited here describe methods that can be programmed using computer algebra software (CAS), but none of them provide software that is independent of them. The only referenced software that meets this requirement is the program ODKIL [32], which is written in FORTRAN and only allows for floating point computations.

The Riccati-Padé method (RPM) [33–39] is a very straightforward method to solve the Schrödinger equation and related eigenvalue problems that consists in writing a Riccati equation for the derivative of the logarithm of the wave function and using increasingly large Padé

approximants to represent it, in such a way that the Taylor expansion of both the exact solution and the Padé approximant coincides up to one extra coefficient than the definition of Padé approximant accounts for. This leads to a quantization condition that involves finding the root of the determinant of a Hankel matrix built with the expansion coefficients. The RPM can be programmed with very little effort using a CAS, and it has a very fast rate of convergence to the eigenvalues of the Schrödinger equation and related problems [40–42]. In the present work we provide an efficient implementation of the RPM to solve the Schrödinger equation for the H_2^+ that is independent of CAS. We use our implementation to thoroughly test the convergence properties of the RPM, and we compute the spectrum of 69 different states to 8 – 25 digits of accuracy. We select a few of those states and perform computations with 60 – 100 digits of accuracy; these results may be used as benchmarks for testing other methods. Finally, we analyze the spectra we computed and identify the bound states; we compute the internuclear distance, electronic energy, and separation constant to ~ 40 digits of accuracy. For the ground state, this computation is refined to produce 160 significant digits. We briefly describe the software that allowed such computations, which is distributed under a free software license.

II. THE METHOD

The RPM has been thoroughly described in previous works [33–39, 41–44], but for the sake of completeness we briefly recall its main features here. We also revisit the main generalities of the Schrödinger equation for H_2^+ , and detail the application of the RPM to solve it.

The RPM for coupled equations

The Schrödinger equation and related problems can usually be written in the following manner,

$$L''(x) + P(x)L'(x) + Q(x)L(x) = 0. \quad (1)$$

where $P(x)$ and $Q(x)$ are arbitrary functions that admit expansions in powers of x , $P(x) = \sum_{k=-1}^{\infty} p_k x^k$, and $Q(x) = \sum_{k=-2}^{\infty} q_k x^k$ and depend on one or more parameters λ_i . In the case of the one-dimensional Schrödinger equation, for example, $P(x) = 0$, and $Q(x) = 2E - V(x)$. If $L(x) \sim x^s$ when $x \rightarrow 0$, with s being an integer number, then the regularized logarithmic derivative of L , i.e., the function

$$f(x) = \frac{s}{x} - \frac{L'(x)}{L(x)}, \quad (2)$$

can be expanded in a Taylor series around $x = 0$, i.e., $f(x) = \sum f_j x^j$, and satisfies the following Riccati equation,

$$f'(x) + \left[\frac{2s}{x} + P(x) \right] f(x) - f^2(x) - \frac{s}{x} P(x) - Q(x) - \frac{s(s-1)}{x} = 0. \quad (3)$$

A recurrence relation can be found that relates each f_j with the preceding f_0, \dots, f_{j-1} , and these also depend on the same parameters as $Q(x)$ and $P(x)$.

We now consider an $[M/N]$ Padé approximant to $f(x)$, i.e., a quotient of polynomials of degrees M and N ,

$$[M/N](x) = \frac{\sum_{j=0}^M a_j x^j}{1 + \sum_{k=1}^N b_k x^k}, \quad (4)$$

such that the series expansion of both $f(x)$ and $[M/N](x)$ coincide up to order $M + N + 1$. To each function $f(x)$, there is a unique $[M/N]$ Padé approximant, and there is a set of $M + N$ linear equations that relate the coefficients a_j , and b_j with the f_j coefficients. The RPM consists in choosing the parameters on which P and Q depend in such a way that $[M/N]$ matches an extra coefficient f_j , i.e., $[M/N](x) - f(x) = O(x^{M+N+2})$. This adds an extra equation to the set of $M + N$ ones, and it is straightforward to show that this set has a non-trivial solution if

$$H_D^d(\lambda_1, \dots, \lambda_n) = \begin{vmatrix} f_{d+1} & f_{d+2} & \cdots & f_{d+D} \\ f_{d+2} & f_{d+3} & \cdots & f_{d+D+1} \\ \vdots & \vdots & \ddots & \vdots \\ f_{d+D} & f_{d+D+1} & \cdots & f_{2D+d-1} \end{vmatrix} = 0, \quad (5)$$

where we have defined $D = N + 1$, and $d = M - N$.

Eq. (5) provides a quantization condition for one of the parameters $\lambda_1, \dots, \lambda_n$ and allows to obtain it in terms of the others. For example, in the case of the one-dimensional Schrödinger equation, if the Hamiltonian depends on one parameter, then one can obtain the energy in terms of it, or the values of said parameter for which the energy adopts a particular value, as in the case of the critical parameters[45]. In the case of coupled equations (which is of concern in the present work), one should have as many coupled equations as unknown parameters, and Eq. (5) should be solved simultaneously for each of the equations. The quantization condition (5) is known to yield both the bound states and resonances of many problems in Quantum Mechanics, and it is believed it does so by sending a movable pole at complex infinity [46]. The singularity can be moved around any path in the complex plane, meaning that Eq. (5) also gives solution to both kinds of problems without specifying the boundary conditions [40, 43].

Application to the eigenenergies of the H_2^+ molecule-ion

Within the Born-Oppenheimer approximation, the electronic Hamiltonian for the H_2^+ molecule is,

$$H_{\text{mol}} = -\frac{1}{2}\nabla^2 - \frac{1}{r_1} - \frac{1}{r_2}, \quad (6)$$

where ∇ involves differentiation with respect to the electron coordinates, and $r_{1,2}$ are the absolute distances between the electron and each of the nuclei. Here atomic units are being used. The Schrödinger equation defined by Eq. (6) can be transformed into a set of separable equations by using the spheroidal coordinates λ, μ and ϕ , where λ and μ are defined as

$$\lambda = \frac{r_1 + r_2}{R}, 1 \leq \lambda < \infty, \quad (7)$$

$$\mu = \frac{r_1 - r_2}{R}, -1 \leq \mu \leq 1, \quad (8)$$

and $0 \leq \phi \leq 2\pi$ is the angle of rotation of the electron around the internuclear axis. R is the internuclear separation, also in atomic units. The electronic wavefunction can be written as a product $\psi(\lambda, \mu, \phi) = L(\lambda)M(\mu)\Phi(\phi)$, and satisfies the following equations:

$$\Phi(\phi) = \frac{1}{\sqrt{2\pi}}e^{im\phi}, \quad m = 0, \pm 1, \pm 2, \dots, \quad (9)$$

$$\frac{d}{d\lambda} \left[(\lambda^2 - 1) \frac{dL(\lambda)}{d\lambda} \right] + \left[-\frac{m^2}{\lambda^2 - 1} - \epsilon\lambda^2 + 2R\lambda + A \right] L(\lambda) = 0 \quad (10)$$

$$\frac{d}{d\mu} [(1 - \mu^2)] + \left[-\frac{m^2}{1 - \mu^2} + \epsilon\mu^2 - A \right] M(\mu) = 0, \quad (11)$$

where A is the separation constant, $\epsilon = -R^2E/2$, with E being the electronic energy i.e., the eigenvalue of H_{mol} , and m is the quantum number associated with the angular momentum in the direction of the internuclear axis.

In order to solve Eqs. (10) and (11) with the RPM, we first define $x = \lambda - 1$, which transforms Eq. (10) into Eq. (1), with

$$P_\lambda(x) = \frac{2(x+1)}{x(x+2)}, \quad (12)$$

$$Q_\lambda(x) = \frac{2R(x+1) + A - \epsilon(x+1)^2}{x(x+2)} - \frac{m^2}{x^2(x+2)^2}.$$

The solution $L(x)$ is known to behave at origin as $x^{|m|/2}$; then by setting $s = |m|/2$ in Eq. (2) we remove the singularities of Eq. (1) at origin, and writing $f(x) = \sum_{j=-1}^{\infty} f_j x^{j+1}$, the following

recurrence relation for the coefficients f_j is obtained,

$$f_{-1} = \frac{2s^2 + s - \epsilon + 2R + A}{2(2s + 1)},$$

$$f_j = \frac{1}{n + 2s + p_{-1}^\lambda + 1} \left[\sum_{k=0}^j (f_{k-1}f_{j-k-1} - p_k^\lambda f_{j-k-1} + sp_{k+1}^\lambda) + q_j^\lambda \right], j = 0, 1, \dots, \quad (13)$$

where p_j^λ and q_j^λ are the expansion coefficients for $P_\lambda(x)$ and $Q_\lambda(x)$.

Similarly, by setting $\mu = x$, Eq. (11) transforms into Eq. (1), with

$$P_\mu(y) = -2x/(1 - x^2),$$

$$Q_\mu(y) = \frac{\epsilon x^2 - A}{1 - x^2} - \frac{m^2}{(1 - x^2)^2}. \quad (14)$$

Now we define

$$g(x) = \frac{t}{x} - \frac{M'(x)}{M(x)}. \quad (15)$$

Since $P_\mu(x)$ is odd and $Q_\mu(x)$ is even, $M(x)$ has defined parity. Therefore, $P_\mu(x) = \sum_{j=0}^{\infty} p_j^\mu x^{2j+1}$, $Q_\mu(x) = \sum_{j=0}^{\infty} q_j^\mu x^{2j}$, and $g(x) = \sum_{j=0}^{\infty} g_j x^{2j+t}$, where $t = 0$ for even states and 1 for odd states, and the following recurrence relation is obtained:

$$g_j = \frac{1}{2j + 2t + 1} \left[\sum_{k=0}^j (f_k f_{j-k-1} - p_k^\mu f_{j-k-1}) + t p_j^\mu + q_j^\mu \right], \quad j = 0, 1, 2, \dots \quad (16)$$

The RPM quantization condition (5) becomes

$$H_{\mu,D}^d(\epsilon, A) = H_{\lambda,D}^d(\epsilon, A, R) = 0. \quad (17)$$

There are three unknowns and only two equations; consequently, equations (10) and (11) yield two parameters in terms of the third one. For benchmarking purposes, it is customary to solve for ϵ and A in terms of R .

Computation of the Hankel determinants and their roots

Any computer algebra system (CAS) contains subroutines to compute the determinant of a matrix. These subroutines are usually good enough for general purposes, but they don't exploit the recurrence relation obeyed by the Hankel matrices that provides a much more efficient way to compute them,

$$H_D^d = \frac{H_{D-1}^d H_{D-1}^{d+2} - (H_{D-1}^{d+1})^2}{H_{D-2}^{d+2}}, \quad (18)$$

$$\begin{array}{ccccccccccc}
f_3 & f_4 & f_5 & f_6 & f_7 & f_8 & f_9 & f_{10} & f_{11} & & \\
H_2^2 & H_2^3 & H_2^4 & H_2^5 & H_2^6 & H_2^7 & H_2^8 & & & & \\
H_3^2 & H_3^3 & \mathbf{H_3^4} & H_3^5 & H_3^6 & & & & & & \\
\mathbf{H_4^2} & \mathbf{H_4^3} & \mathbf{H_4^4} & & & & & & & & \\
\mathbf{H_5^2} & & & & & & & & & &
\end{array}$$

FIG. 1. Sequence of Hankel determinants needed to compute H_5^2 . The subset of determinants required for the last step are marked in bold. Only two consecutive rows need to be stored in memory at the same time.

where $H_1^d = f_{d+1}$, and we define $H_0^d = 1$. To use Eq. (18), we start by computing coefficients $f_{d+1}, \dots, f_{2D+d-1}$. Then, we use them to compute $H_2^d, \dots, H_2^{2D+d-4}$; these are used to compute $H_3^d, \dots, H_3^{2D+d-6}$, and so on, until we reach H_D^d . Since only determinants of order $D-1$ and $D-2$ are needed to compute determinants of order D , for each step we only need to store two rows of determinants in memory. As an example, Figure 1 shows the sequence of determinants required to compute H_5^2 .

Now we discuss the issue of solving Eqs. (17), i.e., finding the roots of the Hankel determinants. To that end, we resort to the well-known Newton-Raphson (NR) method, using numerical differentiation in the form of the symmetric difference quotient. One difficulty that may arise when finding the roots of the Hankel determinants is that H_D^d presents multiple roots that approach to the eigenvalues of the problem [36, 39]. The reason for this is hinted at Eq. (18), by realizing that one solution for $H_D^d = 0$ is $H_{D-1}^d H_{D-1}^{d+2} = (H_{D-1}^{d+1})^2$, but also if both H_{D-1}^d , H_{D-1}^{d+2} , and H_{D-1}^{d+1} are close enough to 0 (they should be, since they are themselves the roots of another Hankel determinant), H_D^d may also become 0. It is typically observed that different sequences of roots converge towards the desired eigenvalues with different speed; we call the fastest of them the “main sequence”. If the starting values provided for the NR method are not good enough it may converge to roots that are not in the main sequence, and for increasing D , the sequence of roots of H_D^d may converge more slowly towards the desired eigenvalue. Besides, it is a well-known fact that the convergence of the NR method deteriorates when dealing with multiple roots. Despite these issues, we have been able to successfully compute the roots of the Hankel determinants for other problems in the past, and for the problem described here in particular, as will be shown below.

The simultaneous solution of Eqs. (17) allows for two different approaches. One of them is to choose a desired value of R , and then solve both equations simultaneously for ϵ and A . This implies solving a system of two equations with two unknowns, for which the NR method is very well suited,

but each iteration of the method involves the evaluation of four derivatives. The other one is to set a value of ϵ , then solve $H_{\mu,D}^d(\epsilon, A)$ to get the corresponding value of A , and solve $H_{\lambda,D}^d(\epsilon, A, R) = 0$ for the value of R . The latter approach has the advantage that it is only required to solve two separate equations, instead of solving them simultaneously, so that it is only necessary to perform one differentiation per iteration for each equation. Unfortunately, the utility of the latter method is limited, since for benchmarking purposes it is usually more desirable to compute ϵ and A values for selected values of R . In the present work we will use both approaches with different purposes, as discussed in the following sections.

The software developed to compute the roots of the Hankel determinants for the H_2^+ molecule is made available under a free software license; its location is disclosed in the Supplementary Material section below.

III. RESULTS

In this section we analyze the rate at which the roots of Eqs. (17) converge towards the values of the energy and separation constant. We then compute the dissociation curves for 69 states; from those curves we identify the bound states and compute the equilibrium internuclear distance, electronic plus nuclear energy, and separation constants to unprecedented accuracy. We also provide accurate benchmark values of the electronic energy and separation constant for 21 states at a fixed internuclear distance.

Convergence of the roots of the Hankel determinants

We first turn our attention to the rate at which the solutions of Eqs. (17) converge towards the correct values of A and ϵ for different values of R . To do so, we first set a value of R ($= 1, 2, 5, 10, 20, 50$, or 90), and then we pick an approximate value of the electronic energy E from Ref. [5] (the use of literature values is not strictly required, as discussed in the following section, but facilitates our work). We then compute $\epsilon = -R^2 E/2$ and solve $H_{D,\mu}^0(\epsilon, A) = 0$ for increasing values of D (using $d = 1, 2$ gives similar results). To measure the convergence rate, we plot $\Delta = \log_{10} |(A[D, 0] - A[D-1, 0])/A[D, 0]|$ against D , where $A[D, d]$ is the value of A computed by solving $H_{\lambda,D}^d = 0$. This plot gives a good approximation to the number of significant digits in the result. We proceed similarly to measure the convergence rate of the roots of $H_{\lambda,D}^0$ towards the value of ϵ that corresponds to the value of R chosen at the beginning and the corresponding value

of A computed with $H_{\mu,D}^0 = 0$. We repeated this procedure for the states $1s\sigma_g$, $2p\sigma_u$, $2p\pi_u$, and $3d\delta_g$, which are the states with the lowest energy for the sets of quantum numbers (m, s) equal to $(0, 0)$, $(0, 1)$, $(1, 0)$, and $(1, 1)$, respectively. The plots of Δ vs D for the μ - and λ - equations are shown in Figs. 2 and 3, respectively.

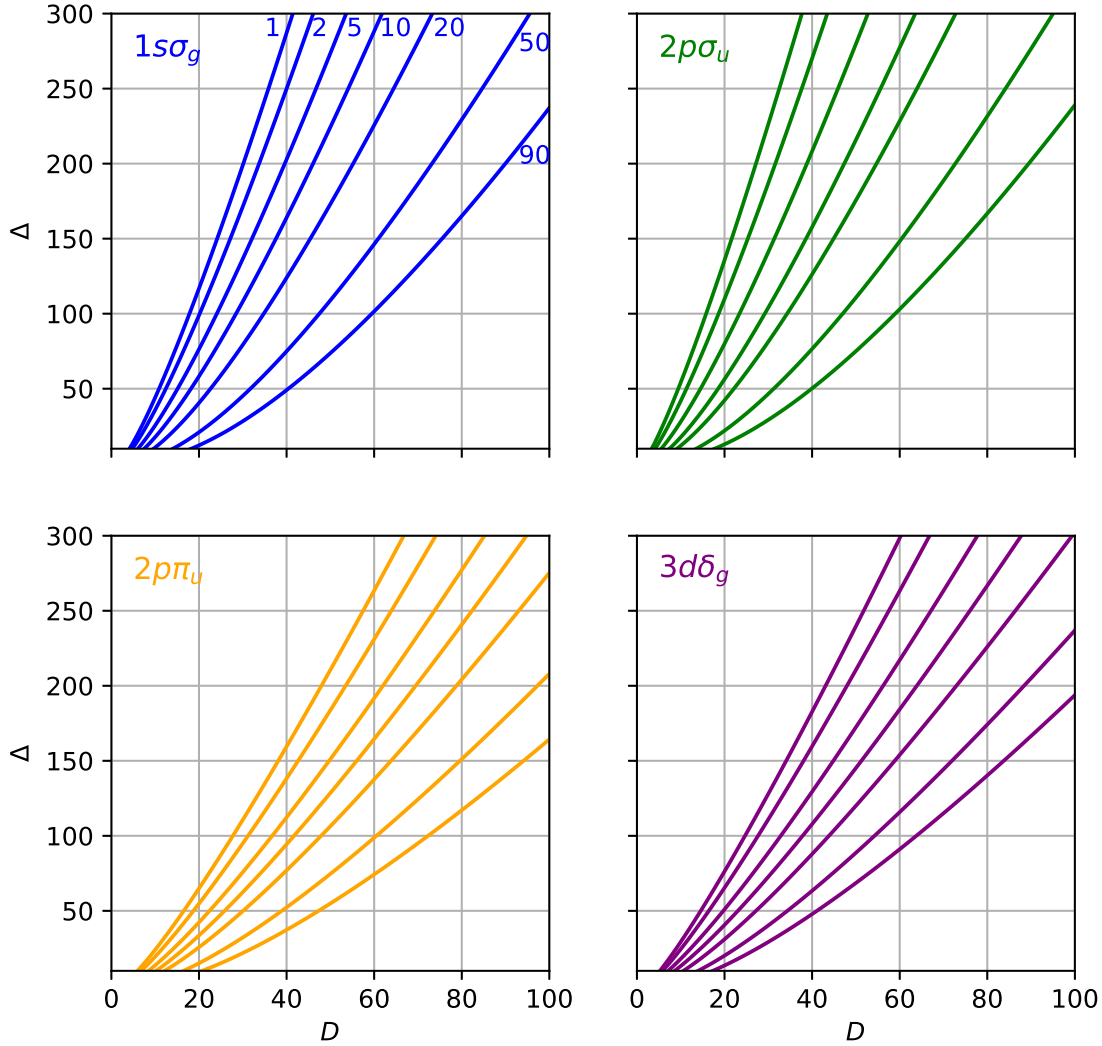


FIG. 2. Convergence of the roots of $H_{\mu,D}^0 = 0$ towards the correct value of A for different values of ϵ in different states. Here, $\Delta = -\log_{10} |(A[D, 0] - A[D - 1, 0])/A[D, 0]|$ is shown. For each graph, the lines from left to right correspond to ϵ values such that $R = 1, 2, 5, 10, 20, 50, 90$ (the values of R are shown next to each line for the state $1s\sigma_g$, and for the other states it follows the same order).

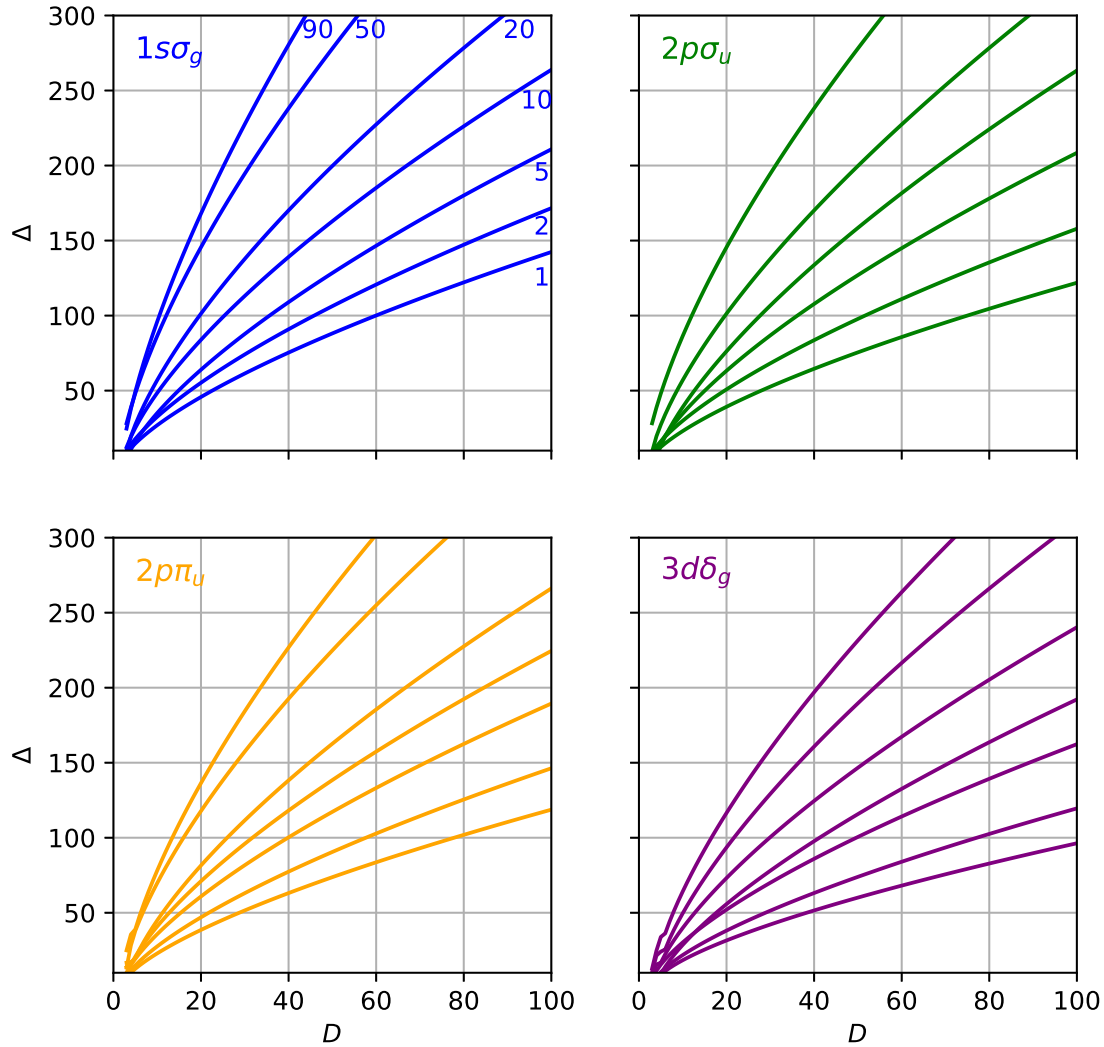


FIG. 3. Convergence of the roots of $H_{\lambda, D}^0 = 0$ towards the correct value of R for different values of ϵ in different states. Here, $\Delta = -\log_{10} |(R[D, 0] - R[D - 1, 0]) / R[D, 0]|$ is shown. For each graph, the lines from right to left correspond to ϵ values such that $R = 1, 2, 5, 10, 20, 50$, and 90 (the values of R are shown next to each line for the state $1s\sigma_g$, and for the other states it follows the same order).

Figure 2 shows that for the four states analyzed, the smaller the values of R (or ϵ), the greater the rate of convergence. Remarkably, the later is faster than exponential, since the plot of the logarithmic difference between iterations is convex. An analysis of the plot for ϵ leads to the opposite conclusion, i.e., convergence rate is slower than exponential, and it increases for larger R .

The result is that for larger (or smaller) values of R , solving both of equations (17) simultaneously can become more difficult, since the solution of one of the equations converges faster than the other one. Despite this, for the lower-lying states, convergence speed of both equations is fast enough to obtain accurate results without great computational effort, as shown in the following sections.

Computation of the spectrum of H_2^+

As discussed before, for the NR method to converge towards the roots of the Hankel determinants, it is important to provide good initial values. This usually implies computing approximate values using another method or looking them up in literature, but for this particular problem we have designed a very simple algorithm that allows to compute the electronic energy for any state of the H_2^+ molecule without resorting to external references. To do so, it takes advantage of the fact that when $R = 0$, both nuclei merge, transforming the system into He^+ , whose Schrödinger equation can be solved exactly. We refer to this case as the united-atom (UA) limit. The eigenvalue E in the UA limit is equal to $-2/n_u^2$, where n_u is the quantum number (note that n_u is a “good” quantum number only in this limit). To identify each state for general R and relate it to the UA ones, we follow Ref. [3] in using the quantum number m , and the “quantum numbers” l and I . Here l is the angular quantum number of the UA solution, and $I = n_u - l$ distinguishes states with the same l but different n_u . The numbers of nodes of the solutions of equations (10) and (11) (N_λ and N_μ) are related to I and l according to $N_\lambda = I - 1$, and $N_\mu = |l - m|$. As stated before, when computing the Hankel determinants, s must be set to $|m|/2$, and t must be set equal to 0 if N_μ is even, and to 1 if N_μ is odd. The separation constant A in the UA limit is $A = -l(l + 1)$ [31].

To compute the whole energy curve (and its corresponding separation constants), we begin from the UA limit ($R = 0$), computing the corresponding values of E and A using the exact formulas. Then, we set $R \leftarrow R + \delta$, and use these values of E and A as starting points for the NR method to solve Eqs. (17) simultaneously, with $D = D_{\min}$, with D_{\min} originally set to 5. The result is used as a starting point for $D = D_{\min} + 1$, and so on, until $D = D_{\min} + 10$. This yields results with a varying number of significant digits, depending on the rate at which Eqs. (17) converge towards the correct values, which can fluctuate significantly, as shown in Figs. 2 and 3. By comparing the amount of digits that coincide between the roots of Eqs. (17) for two subsequent values of D , one can estimate the number of digits of a given approximate result that are correct. For a given value of D , the Hankel determinant may not be large enough that its roots give an approximation to a particular state. For increasing N_λ and N_μ , usually larger values of D are required, and if using

a smaller value, the NR method converges to an approximation of a different state, or does not converge at all. This can be easily accounted for by comparing the converged result with the initial value provided to the NR method. If the relative difference between these values is greater than a set threshold, then the computation is repeated using a larger value of D_{\min} . The new values $E(R+\delta)$ and $A(R+\delta)$ can be used as starting values for $R+2\delta$, and the procedure is repeated until the desired values of R are covered. For a given R , too large values of δ make E and A unsuitable starting points for the NR method to find the Hankel determinant roots for $R+\delta$. A much better starting point is provided by extrapolating the three previous values of E and A using a quadratic equation. We have included all the computations we performed in the Supplementary Material, with the correct amount of significant digits. The algorithm described above is also provided under a free software license in the form of a Python script.

Accurate benchmark values for selected cases

As discussed in the Introduction, it is of interest to have accurate benchmark values available, mainly to use them as a test for other methods. Here we compute E and A for some electronic states at particular internuclear distances to a large number of digits. We do so by using as starting points the values computed in the previous section, and improve their accuracy by solving Eqs. (17) for values of D from 2 to 100. Whenever we found that a result was accurate to 100 or more digits, we stopped the calculation to save time. Also, some of the computations were stopped earlier because the NR method was unable to find the roots after 10000 successive iterations. The values provided here may serve as benchmarks for testing other methods, and we would like to reiterate here that results of similar quality can be obtained for different internuclear positions and quantum numbers by using the software provided with the present work. For brevity, the complete results are not presented in this article, but they are provided in the Supplementary Material. Table I has a summary of all the computed states and the number of significant digits provided, maximum value of D reached, and approximate values of E and A .

Bound states and the location of their minima

Within the Born-Oppenheimer approximation, a minimum of a potential-energy curve is a necessary condition for bound states.

$$U(R) = E(R) + \frac{1}{R}. \tag{19}$$

State	R	E_e	A	Digits	D_{\max}
$2p\sigma_u$	2	-0.667534392202383	-1.186889392359195	98	100
$6p\sigma_u$	10	-0.049370966780030	-0.478090183465735	100	100
$5s\sigma_g$	10	-0.051428455005144	0.962222230928367	100	98
$6f\sigma_u$	8	-0.066255008265486	-10.930552412011943	100	97
$6d\pi_g$	10	-0.051519882071881	-4.869986869409223	100	96
$3d\pi_g$	4	-0.230953442309872	-5.194805350517823	100	93
$5p\pi_u$	10	-0.057271824571940	-1.386797316468034	100	93
$6d\sigma_g$	10	-0.060074021734383	-4.529352507666266	100	92
$1s\sigma_g$	2	-1.102634214494946	0.811729584624757	100	91
$3d\sigma_g$	4	-0.285723790479775	-4.860858109730897	100	90
$5d\delta_g$	10	-0.062792214839847	-5.531151234693738	100	90
$8h\sigma_u$	10	-0.032657740020992	-29.179586335030141	91	90
$5g\phi_g$	8	-0.077751893406662	-19.312733629824027	100	87
$5f\phi_u$	10	-0.067512161659874	-11.613031675139453	100	86
$6h\gamma_u$	10	-0.053894253760732	-29.371445454399158	100	85
$5g\gamma_g$	10	-0.071215504372313	-19.668697103247155	100	82
$8k\delta_u$	10	-0.031625825783903	-55.263865892094628	89	79
$10m\sigma_u$	10	-0.020119384615596	-89.495966943427064	80	71
$7i\delta_g$	10	-0.041602604901644	-41.056025671887276	80	64
$7i\sigma_g$	8	-0.041539060710879	-41.332737524441718	73	63
$9l\sigma_g$	10	-0.024922262061950	-71.375453234003473	69	57

TABLE I. Benchmark states computed in this work. The full numbers with the indicated number of significant digits are provided in the Supplementary Material.

By inspecting several of the plots of $U(R)$ for different states, it is easy to realize that several of them exhibit a minimum. Fig. 4 shows $U(R)$ for all the binding states computed in the present work, with the exception of the ground state. As stated in Ref. [39], equilibrium distances, energies, and separation constants, can be computed by means of the RPM by solving the additional equation

$$\frac{\partial F}{\partial A} \frac{\partial G}{\partial R} - \frac{\partial F}{\partial R} \frac{\partial G}{\partial A} = 0, \quad (20)$$

where $F(U, A, R) = H_{\mu, D}^d(U, A, R)$, and $G(U, A, R) = H_{\lambda, D}^d(U, A, R)$.

Therefore, to obtain the equilibrium energy U_{eq} , separation constant A_{eq} , and internuclear distance R_{eq} , we solve Eqs. (17) and (20) simultaneously. For the ground state, we found that it is better to solve instead for $H_{\lambda, 2D}^d(U, A, R)$, since, for this particular set of parameters, the roots of the Hankel determinants converge faster towards the solution of Eq. (11) than Eq. (10). Analyzing

those solutions with $D \leq 100$ for $d = 0, 1$, and 2 , we get the following results for the ground state:

$$\begin{aligned}
 U_{\text{eq}} &= -0.6026346191065398787275621562899479553992346953448354728 \\
 &\quad 77071864391547692204240182928548052208107736708904195627167 \\
 &\quad 542817913729056948087124900979582036210907045942873, \\
 A_{\text{eq}} &= 0.8097945123220959277383940439312982739965337543254855548957 \\
 &\quad 26033206922628298959352111245158077673262223968225599542440 \\
 &\quad 9412145709954470705258139785977372209240315698, \\
 R_{\text{eq}} &= 1.9971933199699921200682981412764698139402981873092336045912 \\
 &\quad 15197873160737510275851945297613902218158798556730647200620 \\
 &\quad 903944890612509331375201735299111630413056993.
 \end{aligned} \tag{21}$$

We performed similar computations with $D \leq 50$ for the other bound states, and tabulated the results with 10 significant digits in Table II. The same results are provided with 40 significant digits in the Supplementary Material.

State	R	U	A
$1s\sigma_g$	1.997193320 [0]	-6.026346191 [-1]	8.097945123 [-1]
$2p\pi_u$	7.930714973 [0]	-1.345138166 [-1]	2.069815258 [-2]
$3d\sigma_g$	8.834164503 [0]	-1.750490359 [-1]	-1.564171919 [0]
$4d\sigma_g$	1.784921705 [+1]	-5.882062666 [-2]	4.217727831 [-1]
$3d\delta_g$	1.796959858 [+1]	-5.703350664 [-2]	-2.472110245 [0]
$4f\sigma_u$	2.092104113 [+1]	-1.306550866 [-1]	7.116425073 [0]
$4f\pi_u$	1.860780308 [+1]	-7.124680574 [-2]	-3.676755591 [0]
$5f\pi_u$	3.145525562 [+1]	-3.250735500 [-2]	-9.612135220 [-1]
$4f\phi_u$	3.247412486 [+1]	-3.125685627 [-2]	-6.579295566 [0]
$5g\sigma_g$	2.390026713 [+1]	-7.824535362 [-2]	-5.361351964 [0]
$6g\sigma_g$	1.784921705 [+1]	-5.882062666 [-2]	4.217727831 [-1]
$7g\sigma_g$	4.930661152 [+1]	-2.073678351 [-2]	-9.820801505 [-1]
$5g\pi_g$	3.565684224 [+1]	-5.826796664 [-2]	4.741584744 [0]
$5g\delta_g$	3.187986608 [+1]	-3.789816631 [-2]	-7.523979396 [0]
$6g\delta_g$	4.873174244 [+1]	-2.049852479 [-2]	-4.156610538 [0]
$5g\gamma_g$	5.259706948 [+1]	-1.968258155 [-2]	-1.187068111 [+1]
$6h\sigma_u$	4.052059034 [+1]	-6.063995570 [-2]	1.367594640 [0]
$7h\sigma_u$	5.608146571 [+1]	-3.267896081 [-2]	5.566063982 [0]
$7h\pi_u$	5.206921423 [+1]	-2.348082158 [-2]	-6.403536162 [0]
$6h\delta_u$	5.416040079 [+1]	-3.270396067 [-2]	1.275260459 [0]
$6h\phi_u$	4.864109832 [+1]	-2.331786680 [-2]	-1.315803003 [+1]
$7i\sigma_g$	4.736111515 [+1]	-4.359696188 [-2]	-1.044102614 [+1]
$8i\sigma_g$	5.967581513 [+1]	-2.548646137 [-2]	-9.572462260 [0]
$7i\pi_g$	5.976836885 [+1]	-3.420356813 [-2]	-2.353500275 [0]
$8i\pi_g$	8.007299332 [+1]	-2.084069028 [-2]	4.351689330 [0]
$7i\delta_g$	5.777185203 [+1]	-2.554026774 [-2]	-1.312927871 [+1]
$8k\sigma_u$	6.817053314 [+1]	-3.519971544 [-2]	-5.100872001 [0]
$9k\sigma_u$	8.454856343 [+1]	-2.180988002 [-2]	-3.351375902 [0]
$8k\pi_u$	6.832548194 [+1]	-2.682656672 [-2]	-1.427116244 [+1]
$8k\delta_u$	8.250740043 [+1]	-2.184692793 [-2]	-7.499062644 [0]
$9l\sigma_g$	7.923408151 [+1]	-2.762761613 [-2]	-1.675602404 [+1]
$9l\pi_g$	9.261849778 [+1]	-2.255205664 [-2]	-9.869012272 [0]

TABLE II. Equilibrium internuclear distance (R), energy (U), and separation constant (A) of all the bound states computed in the present work. The values between brackets indicate the power of ten by which results must be multiplied. The same table is provided with 40 significant digits in the Supplementary Material.

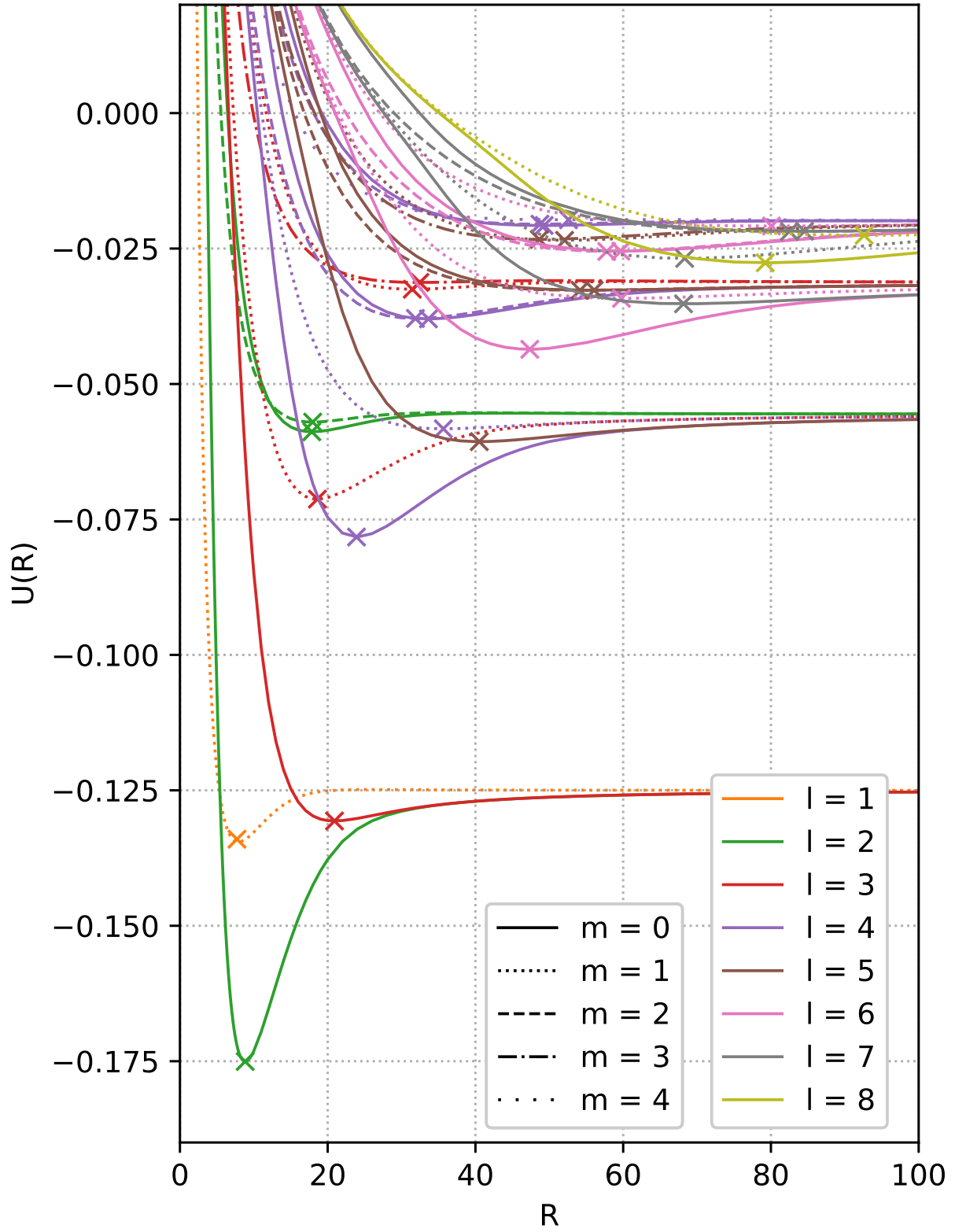


FIG. 4. All the bound states computed in the present work, excluding the ground state. The equilibrium distance for each state is marked with an x.

CONCLUSIONS

We have shown that the RPM is able to compute the eigenenergies and separation constants of the H_2^+ ion-molecule very accurately. The values of the electronic energy and the separation constant for selected values of the internuclear distance for 69 states are provided, as well as the equilibrium parameters for 32 bound states. The code used to perform these computations is also provided, and results of similar accuracy can be obtained for other eigenstates. The scripts used to perform the computations discussed here for the spectra different values of R , starting from $R = 0$, are provided as well. To our knowledge, this is the first time computations of such accuracy are performed for this particular problem, and therefore suggest the results presented here are used as benchmarks for testing other numerical/quantum-mechanical methods.

SUPPLEMENTARY MATERIAL

A data set collection of computational results is available in Zenodo and can be accessed via <https://doi.org/10.5281/zenodo.5044229>. The software used for the computations performed in the present work is also available in Zenodo and can be accessed via <https://doi.org/10.5281/zenodo.5044229>.

-
- [1] D. R. Bates, K. Ledsham, and A. L. Stewart, "Wave functions of the hydrogen molecular ion," *Philosophical Transactions of the Royal Society of London. Series A, Mathematical and Physical Sciences*, vol. 246, pp. 215–240, nov 1953.
 - [2] J. M. Peek, "Eigenparameters for the $1s\sigma_g$ and $2p\sigma_u$ orbitals of H_2^+ ," *The Journal of Chemical Physics*, vol. 43, pp. 3004–3006, nov 1965.
 - [3] D. Bates and R. Reid, "Electronic eigenenergies of the hydrogen molecular ion," in *Advances in Atomic and Molecular Physics*, pp. 13–35, Elsevier, 1968.
 - [4] C. L. Beckel, B. D. Hansen, and J. M. Peek, "Theoretical study of H_2^+ ground electronic state spectroscopic properties," *The Journal of Chemical Physics*, vol. 53, pp. 3681–3690, nov 1970.
 - [5] M. M. Madsen and J. M. Peek, "Eigenparameters for the lowest twenty electronic states of the hydrogen molecule ion," *Atomic Data and Nuclear Data Tables*, vol. 2, pp. IN3–204, dec 1970.
 - [6] P. Okun and K. Burke, "Uncommonly accurate energies for the general quartic oscillator," *International Journal of Quantum Chemistry*, vol. 121, dec 2020.
 - [7] A. V. Turbiner and J. C. del Valle, "Comment on: Uncommonly accurate energies for the general quartic oscillator, Int. J. Quantum Chem., e26554 (2020), by P.Okun and K.Burke," *arXiv e-prints*, p. arXiv:2102.09246, Feb. 2021.

- [8] M. Braun, "Finite element calculations for systems with multiple coulomb centers," *Journal of Computational and Applied Mathematics*, vol. 236, pp. 4840–4845, dec 2012.
- [9] D. M. Chipman and J. O. Hirschfelder, "Perturbation theories for the calculation of molecular interaction energies. II. application to H_2^+ ," *The Journal of Chemical Physics*, vol. 59, pp. 2838–2857, sep 1973.
- [10] B. Jeziorski, K. Szalewicz, and G. Chałasiński, "Symmetry forcing and convergence properties of perturbation expansions for molecular interaction energies," *International Journal of Quantum Chemistry*, vol. 14, pp. 271–287, sep 1978.
- [11] G. Chałasiński and K. Szalewicz, "Degenerate symmetry-adapted perturbation theory. convergence properties of perturbation expansions for excited states of h_2^+ ion," *International Journal of Quantum Chemistry*, vol. 18, pp. 1071–1089, oct 1980.
- [12] S. Yamamoto, Y. Hatano, and H. Tatewaki, "Artificial nodes in the h_2^+ wave functions expanded using gaussian-type orbitals or laguerre-type orbitals," *Computational and Theoretical Chemistry*, vol. 1103, pp. 17–24, mar 2017.
- [13] Y. P. Sarwono, F. U. Rahman, and R. Zhang, "Numerical variational solution of hydrogen molecule and ions using one-dimensional hydrogen as basis functions," *New Journal of Physics*, vol. 22, p. 093059, sep 2020.
- [14] R.-H. Xie and J. Gong, "Simple three-parameter model potential for diatomic systems: From weakly and strongly bound molecules to metastable molecular ions," *Physical Review Letters*, vol. 95, dec 2005.
- [15] J. C. Xie, T. Kar, and R.-H. Xie, "An accurate pair potential function for diatomic systems," *Chemical Physics Letters*, vol. 591, pp. 69–77, jan 2014.
- [16] K. Szalewicz, "Determination of structure and properties of molecular crystals from first principles," *Acc. Chem. Res.*, vol. 47, pp. 3266–3274, 2014.
- [17] M. P. Metz, K. Piszczatowski, and K. Szalewicz, "Automatic generation of intermolecular potential energy surfaces," *Journal of Chemical Theory and Computation*, vol. 12, pp. 5895–5919, dec 2016.
- [18] M. W. Schmidt, J. Ivanic, and K. Ruedenberg, "Covalent bonds are created by the drive of electron waves to lower their kinetic energy through expansion," *The Journal of Chemical Physics*, vol. 140, p. 204104, may 2014.
- [19] M. Beyer and F. Merkt, "Observation and calculation of the quasibound rovibrational levels of the electronic ground state of H_2^+ ," *Physical Review Letters*, vol. 116, feb 2016.
- [20] M. Beyer and F. Merkt, "Structure and dynamics of H_2^+ near the dissociation threshold: A combined experimental and computational investigation," *Journal of Molecular Spectroscopy*, vol. 330, pp. 147–157, dec 2016.
- [21] S. Schiller, I. Kortunov, M. H. Vera, F. Gianturco, and H. da Silva, "Quantum state preparation of homonuclear molecular ions enabled via a cold buffer gas: An ab initio study for the H_2^+ and the D_2^+ case," *Physical Review A*, vol. 95, apr 2017.

- [22] H. Olivares-Pilón and A. V. Turbiner, “The H_2^+ molecular ion: Low-lying states,” *Annals of Physics*, vol. 373, pp. 581–608, oct 2016.
- [23] V. M. Khmara, M. Hnatič, V. Y. Lazur, and O. K. Reity, “Quasicrossings of potential curves in the two-coulomb-center problem,” *The European Physical Journal D*, vol. 72, feb 2018.
- [24] T. J. Price and C. H. Greene, “Semiclassical treatment of high-lying electronic states of H_2^+ ,” *The Journal of Physical Chemistry A*, vol. 122, pp. 8565–8575, oct 2018.
- [25] H. de Oliveira Batael and E. D. Filho, “Excited states for hydrogen ion molecule confined by a prolate spheroidal boxes: variational approach,” *Theoretical Chemistry Accounts*, vol. 139, jul 2020.
- [26] B. D. B. Figueiredo and M. Novello, “Solutions to a spheroidal wave equation,” *Journal of Mathematical Physics*, vol. 34, pp. 3121–3132, jul 1993.
- [27] B. D. B. Figueiredo, “Generalized spheroidal wave equation and limiting cases,” *Journal of Mathematical Physics*, vol. 48, p. 013503, jan 2007.
- [28] R. Boyack and J. Lekner, “Confluent heun functions and separation of variables in spheroidal coordinates,” *Journal of Mathematical Physics*, vol. 52, p. 073517, jul 2011.
- [29] T. Kereselidze, G. Chkadua, and P. Defrance, “Coulomb sturmians in spheroidal coordinates and their application for diatomic molecular calculations,” *Molecular Physics*, vol. 113, pp. 3471–3479, apr 2015.
- [30] T. Kereselidze, G. Chkadua, P. Defrance, and J. F. Ogilvie, “Derivation, properties and application of coulomb sturmians defined in spheroidal coordinates,” *Molecular Physics*, vol. 114, pp. 148–161, oct 2015.
- [31] T. C. Scott, M. Aubert-Frécon, and J. Grotendorst, “New approach for the electronic energies of the hydrogen molecular ion,” *Chemical Physics*, vol. 324, pp. 323–338, may 2006.
- [32] G. Hadinger, M. Aubert-Frecon, and G. Hadinger, “The killingbeck method for the one-electron two-centre problem,” *Journal of Physics B: Atomic, Molecular and Optical Physics*, vol. 22, pp. 697–712, mar 1989.
- [33] F. M. Fernandez, G. I. Frydman, and E. A. Castro, “Tight bounds to the schrodinger equation eigenvalues,” *Journal of Physics A: Mathematical and General*, vol. 22, pp. 641–645, mar 1989.
- [34] F. M. Fernández, Q. Ma, D. J. DeSmet, and R. H. Tipping, “Calculation of energy eigenvalues via supersymmetric quantum mechanics,” *Canadian Journal of Physics*, vol. 67, pp. 931–934, oct 1989.
- [35] F. M. Fernández, Q. Ma, and R. H. Tipping, “Eigenvalues of the schrödinger equation via the riccati-padé method,” *Physical Review A*, vol. 40, pp. 6149–6153, dec 1989.
- [36] F. M. Fernández, Q. Ma, and R. H. Tipping, “Tight upper and lower bounds for energy eigenvalues of the schrödinger equation,” *Physical Review A*, vol. 39, pp. 1605–1609, feb 1989.
- [37] F. M. Fernández, “Strong coupling expansion for anharmonic oscillators and perturbed coulomb potentials,” *Physics Letters A*, vol. 166, pp. 173–176, jun 1992.
- [38] F. M. Fernández, R. Guardiola, and M. Znojil, “Riccati-padé quantization and oscillators $V(r)=gr^\alpha$,” *Physical Review A*, vol. 48, pp. 4170–4174, dec 1993.

- [39] F. M. Fernández, “Alternative treatment of separable quantum-mechanical models: The hydrogen molecular ion,” *The Journal of Chemical Physics*, vol. 103, pp. 6581–6585, oct 1995.
- [40] F. M. Fernández and J. Garcia, “Unitary transformations of a family of two-dimensional anharmonic oscillators,” *Journal of Mathematical Chemistry*, vol. 54, pp. 1321–1326, mar 2016.
- [41] F. M. Fernández and J. Garcia, “Highly accurate calculation of the real and complex eigenvalues of one-dimensional anharmonic oscillators,” *Acta Polytechnica*, vol. 57, p. 391, dec 2017.
- [42] F. M. Fernández and J. Garcia, “Highly accurate calculation of the resonances in the stark effect in hydrogen,” *Applied Mathematics and Computation*, vol. 317, pp. 101–108, jan 2018.
- [43] F. M. Fernández, “Quantization condition for bound and quasibound states,” *Journal of Physics A: Mathematical and General*, vol. 29, pp. 3167–3177, jun 1996.
- [44] F. M. Fernández and J. Garcia, “On two different kinds of resonances in one-dimensional quantum-mechanical models,” *Journal of Mathematical Chemistry*, vol. 55, pp. 623–631, oct 2016.
- [45] F. M. Fernández and J. Garcia, “Local approximation to the critical parameters of quantum wells,” *Applied Mathematics and Computation*, vol. 220, pp. 580–592, sep 2013.
- [46] S. Abbasbandy and C. Bervillier, “Analytic continuation of Taylor series and the boundary value problems of some nonlinear ordinary differential equations,” *Applied Mathematics and Computation*, vol. 218, pp. 2178–2199, nov 2011.